



# Application of response surface method for COD and TOC removal in leachate treatment through hybrid process (coagulation–flocculation/photo-Fenton/extended aeration)

F. Hashemzadeh<sup>1</sup> · S. H. Rahmati<sup>2</sup> · B. Ahangari<sup>3</sup>

Received: 8 June 2022 / Revised: 29 October 2022 / Accepted: 6 November 2022 / Published online: 19 November 2022

© The Author(s) under exclusive licence to Iranian Society of Environmentalists (IRSEN) and Science and Research Branch, Islamic Azad University 2022

## Abstract

In this study, the coagulation and flocculation (CF) process and photo-Fenton (PF) method have been used by examining the TOC and COD parameters in landfill leachate in Mallard, Iran. To optimize the studied parameters, the experimental design was performed in the design-expert software with the response surface method (RSM). At first, experiments related to the CF process were designed using the miscellaneous module, and then, the central composite module was used to experimental design in the PF process. The removal percentage of COD and TOC in the CF process using  $\text{FeCl}_3$  coagulant was obtained to be 30% and 63% at pH 11 and  $100\text{gL}^{-1}$  of  $\text{FeCl}_3$  coagulant, respectively. Afterward, the output was used in the photo-Fenton process. The removal percentage of TOC and COD in the photo-Fenton phase (obtained at pH 7,  $5\text{mgL}^{-1}$  of  $\text{FeSO}_4 \cdot 7\text{H}_2\text{O}$ ,  $3.13\text{mgL}^{-1}$  of  $\text{H}_2\text{O}_2$ , the reaction time of 62.5 min, and voltage of 14 V) was reported to be 34% and 68%, respectively. The correlation coefficients ( $R^2$ ) for fitted models in the CF process were equal to 0.9909 and 0.9261, respectively. In the PF process, the results were 0.9901 and 0.9883 proving the validity of the models presented. Finally extended aeration (EA) was also investigated to evaluate the effect of CF/PF processes which resulted in the 85% removal efficiency of the COD using the combination of CF/PF/EA processes. According to the obtained results, hybrid processes can be considered as an effective option in treating landfill waste leachate.

**Keywords** COD removal · TOC removal · Leachate treatment · Response surface method (RSM) · Coagulation and flocculation process · Photo-Fenton process · Extended aeration · Hybrid process

## Introduction

Significant amounts of waste will still be disposed of in landfills even with the best reduction separation and recycling programs (Veli et al. 2021). Hence, one of the permanent and mandatory components of all waste management

systems whether large or small is final disposal which mainly includes sanitary landfilling (Vilar et al. 2011). Leachate is a liquid that is released due to the entry of water such as rain-water runoff drainage or groundwater into the landfill or can be produced because of water seepage and moisture from inside of the landfill to out of it (Peng 2017). Important and influential factors on leachate quality include waste composition temperature and humidity available oxygen landfill site decomposition stage of organic materials in the waste and most importantly age of the leachate (Singh and Tang 2013). The decomposition of organic material takes place in 5 steps, which, respectively, include the initial adaptation phase transition phase acidic phase methane fermentation phase and supplementary or maturation phase (Jiang et al. 2021). Due to the high activity of acid-producing bacteria, which are categorized as obligate and facultative anaerobes, the leachate produced in the acidic phase decomposes organic material and produces large amounts of acid, which leads to a decrease in the pH of leachate (Mirghorayshi et al.

Editorial responsibility: Samareh Mirkia.

✉ S. H. Rahmati  
drhodarahmati@gmail.com

<sup>1</sup> Researcher at Water and Wastewater Research Center., Water Research Institute(WRI),, Tehran,, Iran

<sup>2</sup> Assistant Professor in Faculty of Natural Resources and Environment, Science and Research Branch,, Islamic Azad University,, Tehran,, Iran

<sup>3</sup> Department of Environmental Health Engineering, School of Public Health and Safety,, Shahid Beheshti University of Medical Sciences,, Tehran,, Iran



2021). This type of leachate contains high concentrations of COD TOC BOD and heavy metal ions and also has high electrical conductivity (EC) (Kurtoğlu, Akkaya, and Bilgili 2020). The leachate produced after entering the methane fermentation phase changes due to the activity of anaerobic microorganisms called methane-forming microorganisms and converts acetic acid and hydrogen gas to methane and carbon dioxide. The amount of produced acid at this stage decreases compared to the previous stage, so the pH will increase (Nain et al. 2021). At this stage, the heavy metal ions in the leachate are deposited and their concentrations decrease due to the increase in solution pH (Kawai et al. 2012). Due to the reduction of biodegradable organic materials, gas production will decrease in the supplementary stage and the amount of humic acid and folic acid will increase. Considering the steps mentioned earlier, it can be concluded that the process of changes in the production of complex organic materials and the reduction of biodegradability can multiply the management problems of leachate produced in the landfill (Liu et al. 2022; Yang et al. 2022).

Waste leachate is classified according to the age of the landfill site and is divided into three categories: old intermediate and young. The qualitative characteristics of each of which are presented in Table 1 (Amor et al. 2015; Tejera et al. 2021).

Leachate pollutions are released from waste because of physical chemical and biological processes (Shi et al. 2021). The produced leachate has the potential to cause many environmental problems. It pollutes the environment when coming in contact with surface water groundwater or the soil around it (Wijekoon et al. 2022).

Municipal solid waste contains a large microbial population and may also be contaminated by pathogenic microorganisms (Zhao et al. 2021). Waste often contains animal waste and carcasses sewage sludge and sometimes hospital waste. Therefore, they are a suitable environment for the growth of pathogenic microorganisms and are considered a serious health risk (Sawamura et al. 2010). Some of the dangerous chemicals identified in leachate include diethyl phthalate, dioctyl phthalate, benzyl butyl phthalate, 2-methyl naphthalene, 2-vinyl naphthalene, naphthalene,

acenaphthylene, acenaphthene, fluorene, and Methoprene, which are categorized as the priority pollutants (Li et al. 2016). Leachate quality determines the treatment process. Due to its high BOD/COD ratio, young leachate has a high biodegradability, so using biological processes will be more justified than other physical and chemical processes (Anna Tałałaj et al. 2021); whereas due to low biodegradability processes such as coagulation and flocculation (Cheng et al. 2021) membrane processes adsorption (Zielińska et al. 2020) and advanced oxidation (Pisharody et al. 2022) should be used for old leachate. Using these methods solely has disadvantages such as the need for high materials and energy and high cost therefore we use hybrid processes to overcome these difficulties (Kusworo et al. 2021). Integration of flocculation and advanced oxidation processes is one of the hybrid processes that has received a lot of attention in recent years (Vedrenne et al. 2012; Li et al. 2016; Mohsen Behnezhad 2021; Wu et al. 2021).

Advanced statistical design is frequently used for characterization optimization and modeling of a specific treatment. Here, in order to investigate correlated factors in the leachate treatment process and their optimization, we used response surface methodology (RSM) a combination of mathematical and statistical tools. The RSM might generate significantly more information from only a small number of experiments than could conventional optimization techniques (Roudi et al. 2021).

In this study, the response surface method (RSM) was used for investigating the mentioned cases and central composite and miscellaneous modules were chosen through others. The advantages of the mentioned methods are examining the effects of different variables on each other and reducing the number of experiments without abridging their statistical validity, which reduces time and costs (Vilar et al. 2011; Singh and Tang 2013; Peng 2017; Jiang et al. 2021).

Carlos Amor et al. first used the coagulation and flocculation process and then the Fenton and Photo-Fenton processes for leachate. Their results indicated that if the coagulation and flocculation process is used before the Fenton process, the COD rate will be reduced by 89% in 96 h and the COD rate is reduced by 75% in the photo-Fenton process (Amor

**Table 1** Qualitative characteristics of leachate types resulting from landfill sites

Parameter	Young landfill leachate (<5 years)	Intermediate landfill leachate (5–10 years)	Mature landfill leachate (> 10 years)
COD	25 – 60gO <sub>2</sub> L <sup>-1</sup>	The characteristics of this type of leachate are between young and old leachate	5–20 gO <sub>2</sub> L <sup>-1</sup>
BOD	4–15 gO <sub>2</sub> L <sup>-1</sup>		0.1–0.2 gO <sub>2</sub> L <sup>-1</sup>
Ammonium nitrogen	0.5–2 gL <sup>-1</sup>		3–5 gL <sup>-1</sup>
BOD/COD	0.5–0.6		<0.1
pH	4		> 7.5

et al. 2015). Jiuyi Li et al. first passed the leachate through nanoporous membranes, and then, further treatment of concentrated material was carried out using coagulation and flocculation process followed by Fenton and photo-Fenton. The results showed that more than 90% of COD and TOC were removed through this process (Li et al. 2016). In addition, Michel Vedrenne et al. first used the coagulation and flocculation process along with photo-Fenton, and then, the resulting supernatant was subjected with the bacterium *Artemia salina* in order to the leachate purification. The removal percentages of TC,  $\text{NH}_4$ , and COD were reported to be 95%, 64%, and 56%, respectively. The amounts of heavy metal ions in the final output were also determined and the removal percentages of lead(II) and arsenic(III) have been reported to be 85% and 49%, respectively (Vedrenne et al. 2012). Andrea Colombo et al. also used the biological process after the photo-Fenton process such that by combining these two processes they were able to bring the amount of waste leachate to the environmental discharge standards (Colombo et al. 2019). Therefore, as shown in Fig. 1 this study was conducted to combine the coagulation and flocculation process along with photo-Fenton and optimization the experiment by response surface methodology (RSM) (a combination of mathematical and statistical technique) to reduce the waste leachate contamination and facilitate its biological treatment.

## Materials and methods

### Characteristics of landfill leachate

Akhtarabad landfill located in Akhtarabad village near Safa Dasht city has an area of 200 hectares, and 5 hectares of it is occupied annually for waste disposal. On average, 700–1000 tons of waste is dumped daily from three cities

**Table 2** Qualitative characteristics of leachate sampled from Akhtarabad landfill

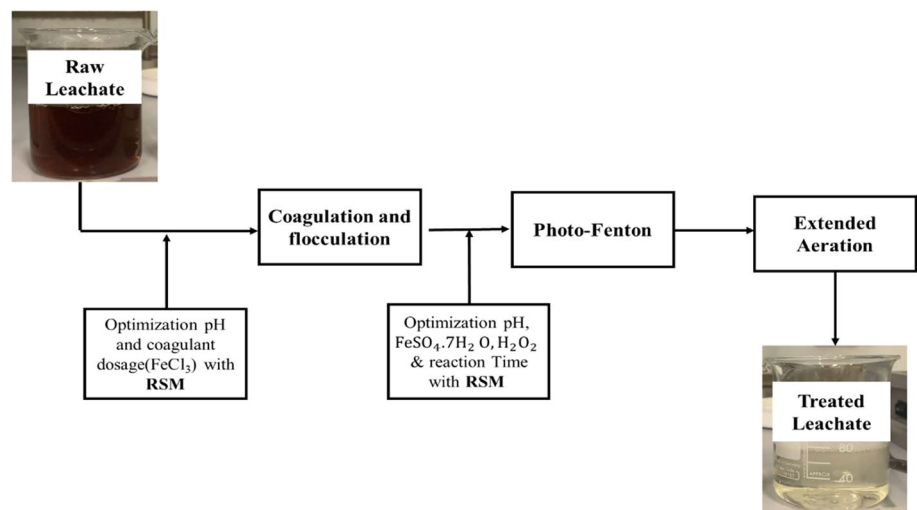
Parameters	Raw leachate
COD	6.2 $\text{gO}_2\text{L}^{-1}$
BOD <sub>5</sub>	0.5 $\text{gO}_2\text{L}^{-1}$
BOD <sub>5</sub> /COD	0.08
Turbidity	0.26 NTU
pH	7.5
TSS	0.18 $\text{gO}_2\text{L}^{-1}$

of Mallard Shahriyar and Quds with a production rate of 800 g per person per day of waste. The amount of moisture in this waste is 68–75%, and the amount of decomposable organic matter is 70%. In this area, 24 springs and 38 aqueducts have been identified that are used for drinking water agriculture and fish and livestock breeding. Due to the high probability of leachate leakage from the landfill to groundwater in this area, it is necessary to consider appropriate methods to reduce pollution or completely decontaminate leachate because some pollutants can directly or indirectly endanger human life health because of their high bioaccumulation properties in living organisms.

In this study, the leachate obtained from Akhtarabad landfill located in Akhtarabad village was collected in polyethylene containers and immediately delivered to the Water and Wastewater Laboratory of the Faculty of Environment and Energy Tehran-Iran Azad University of Research Sciences. To maintain the qualitative characteristics, the samples were kept at 4° C until the experiments were performed (de Moraes and Zamora 2005). To homogenize the qualitative characteristics, the samples were mixed well before the experiments. The leachate properties were measured thrice, and the average values are shown in Table 2.

Based on the obtained results from the analysis, the leachate is of the mature type (Table 1). Therefore, it is not

**Fig. 1** Schematic diagram of the process to treatment leachate of Akhtar Abad landfill



decomposed by conventional biological methods and other physical or chemical procedures must be used.

The chemicals used in this study include  $\text{FeSO}_4 \cdot \text{H}_2\text{O}$  (85%),  $\text{FeCl}_3 \cdot 6\text{H}_2\text{O}$ ,  $\text{H}_2\text{O}_2$  (30% w/w), sulfuric acid (97%), and sodium hydroxide. All of them were in analytical grade and purchased from Merck Company. To weigh chemicals, Sartorius-PRACTUM113-13 digital balance was used. The solution's pH values were fitted by a Grison-2D pH meter. The relative clarity of the solution was measured by a WTW-TURB355 Turbidity meter. The UV–Vis spectra of the solutions were recorded by a DR 5000 spectrophotometer. For uniform stirring of the solutions a JI-M6c jar test device was used. Total organic carbon (TOC) is also determined by a Hatch-DRB: Digital Reactor Block.

All the experiments were conducted in jar test containers (250 ml) at ambient temperature.  $\text{FeCl}_3$  was selected as the coagulant and the experiments were designed by design-expert software using response surface method and 3-level factorial miscellaneous module. The variables investigated in the coagulation and flocculation process including coagulation dosage of 1, 5.05 and 100  $\text{gL}^{-1}$  and pH range of 5–11. A total of 13 experiments with 4 center points (pH = 8 and coagulant dosage = 5.05  $\text{gL}^{-1}$ ) were considered in this study. The experiments are ordered based on Std in order to prevent the alignment of center points and determine the accuracy of laboratory studies. The pH and dosage factors are abbreviated as A and B, respectively. In the response section, removal of TOC and COD is expressed as percentages. The coagulation and flocculation process takes place in three stages, which are fast mixing, slow mixing and precipitation, respectively. In fast mixing, the samples are stirred for 2 min at 150 rpm, then the slow mixing commences at 40 rpm for 20 min, and finally they are allowed to precipitate without stirring for 30 min.

In the next step, photo-Fenton experiments were conducted at room temperature in jar test containers. Software designed 60 experiments with 12 central points for this step. Independent variables were classified into two categories: quantitative and qualitative. Quantitative variables consist of pH range of 3–11, coagulant dosage in the range of 5–60  $\text{mgL}^{-1}$ , 1.25–5% of  $\text{H}_2\text{O}_2$  and reaction time of 5–120 min. Voltage was defined as a qualitative variable because it was evaluated at two levels (14 and 14 + 9 V).

The stated values are placed in 5 levels, which are named +a + 10 – 1 – a for the design experiment. After removing the supernatant from the leachate provided from the previous step, it stirred well and then poured into jar test containers. At first, the pH of the solutions was adjusted by 0.1 M solutions of NaOH and sulfuric acid. Then, after the addition

of  $\text{FeSO}_4 \cdot 7\text{H}_2\text{O}$ , they were stirred at 300 rpm for 5 min to achieve a homogenous solution. After that, by adding hydrogen peroxide, the solution was stirred at 200 rpm for a certain time and UV–Vis light was emitted. In order to prevent the interference effect of hydrogen peroxide in COD analysis solution, pH values increased to 8 and stirred for 25 min at 100 rpm and then the sample was placed in a water bath at 50 °C for 30 min (Vilar et al. 2011).

Separated supernatant was used to measure the COD and TOC removal percentage. For investigating the biological treatability, firstly the sludge from the wastewater treatment plant was placed in Plexiglass activated sludge pilot with an inner diameter of 10 cm and 25 cm of height. Four hundred milliliters of sludge with suspended solids (SS) 0.6–0.8  $\text{kgss/kgCOD}$  and 1–2% dry solids (DS) were poured into the reactor then the supernatant from the photo-Fenton process was added into the reactor up to the volume of 1500 ml. The pH was adjusted to 7, and the amount of oxygen in the reactor was determined by the oxygen probe. The total duration of the experiments was 72 h, and the type of biological treatment system was extensive aeration. In order to determine the COD removal percentage, the reactor was sampled every 24 h.

## Results and discussion

### Coagulation and flocculation process

This process was optimized by the miscellaneous module of the response surface method and used to determine the

**Table 3** Experimental matrix by 3-level factorial design and actual responses in COD and TOC removal (%) in coagulation and flocculation process

Std	Run	Factor 1 A: pH	Factor 2 B: Dosage ( $\text{gL}^{-1}$ )	Response 1 COD removal (%)	Response 2 TOC removal (%)
5	1	8.00	5.05	13	16
9	2	11.00	100.00	30	63
8	3	8.00	100.00	16	18
10	4	8.00	5.05	14	21
2	5	8.00	1.00	9	9
4	6	5.00	5.05	15	19
11	7	8.00	5.05	15	17
1	8	5.00	1.00	8	16
13	9	8.00	5.05	14	29
7	10	5.00	100.00	18	25
12	11	8.00	5.05	13	28
3	12	11.00	1.00	22	47
6	13	11.00	5.05	27	52



**Table 4** ANOVA results for response surface quadratic model for COD removal (%) in coagulation and flocculation process

Source	Sum of squares	df	Mean square	F-value	p-value	
Model	490.74	5	98.15	152.87	<0.0001	Significant
A-pH	240.67	1	240.67	374.85	<0.0001	
B-Dose	104.17	1	104.17	162.24	<0.0001	
AB	1.0000	1	1.0000	1.56	0.2522	
A <sup>2</sup>	139.36	1	139.36	217.06	<0.0001	
B <sup>2</sup>	5.39	1	5.39	8.39	0.0231	
Residual	4.49	7	0.6420			
Lack of Fit	1.69	3	0.5648	0.8068	0.5522	Not significant
Pure error	2.80	4	0.7000			
Cor Total	495.23	12				

optimal values of the mentioned parameters to the COD and TOC removal. Table 3 depicts the test results. According to this table, the highest removal efficiencies of COD and TOC were 30% and 63%, respectively, obtained at pH 11 and 100 gL<sup>-1</sup> of coagulant. Table 3 demonstrates that the percentage of COD and TOC removal has increased with increasing pH and coagulant concentration. Additionally, in acidic pH and low concentrations of coagulant, the difference in removal percentage has been significant and around 40%. However, the percentage of COD removal is only about 30%. Jing Xu et al. stated that in the CF/PF process, which is optimized by the response surface method, in addition to reducing COD and TOC of the leachate, the amount of color was also reduced with 100% of removal percentage at 1 M of H<sub>2</sub>O<sub>2</sub> and 17.5 mM of Fe<sup>2+</sup> (Xu et al. 2017).

In the fit summary section, the cubic vs quadratic model was selected as the best model for determining the COD removal efficiency and the sum of squares, df, the mean square, F-value, and P-value prob > F parameters were 1.67, 2, 0.83, 1.47, and 0.3140, respectively. However, this model is not useful due to the applying a large number of different parameters. Therefore, the model shown as alised is discarded and the proposed model by the system in which the quadratic vs 2FI with the sum of squares, df, mean square, F-value, and P-value prob > F

parameters, respectively, equal to 144.99, 2, 72.45, 112.85, and <0.0001 were considered. In the fit summary section, for the TOC removal the cubic vs quadratic model is the best and the sum of squares, df, mean square, F-value, and P-value prob > F parameters were 4.83, 2, 2.42, 0.053, and 0.9492, respectively. Nevertheless, due to the length of the fitted model for the reasons mentioned earlier, it was discarded and the proposed model by the system, in which the quadratic vs 2FI with the sum of squares, df, mean square, F-value, and P-value prob > F parameters were, respectively, equal to 997.53, 2, 498.76, 14.90, and 0.0030, was considered.

ANOVA analysis was used for graphical analysis in order to investigate the interactions between variables and responses of the experiments (Vilar et al. 2011). This analysis is summarized in Tables 4 and 5 for COD and TOC removal.

The F-value of the model is equal to 152.87, which implies the model is significant. There is only a 0.01% chance that a “F-value Model” this large could occur due to noise. “prob > F” values less than 0.05 indicate that the model terms are significant. In this case, A, B, A<sup>2</sup>, B<sup>2</sup> are significant model terms. The “lack of fit F-value” of 0.81 implies the lack of fit is not significant relative to the pure error. There is a 55.22% chance that a “lack of fit F-value”

**Table 5** ANOVA results for response surface quadratic model for TOC removal (%) in coagulation and flocculation process

Source	Sum of squares	df	Mean square	F-value	p-value	
Model	2936.44	5	587.29	17.54	0.0008	Significant
A-pH	1734.00	1	1734.00	51.80	0.0002	
B-Dose	192.67	1	192.67	5.76	0.0475	
AB	12.25	1	12.25	0.3659	0.5643	
A <sup>2</sup>	954.09	1	954.09	28.50	0.0011	
B <sup>2</sup>	32.19	1	32.19	0.9615	0.3595	
Residual	234.32	7	33.47			
Lack of fit	87.52	3	29.17	0.7950	0.5572	Not significant
Pure error	146.80	4	36.70			
Cor total	3170.77	12				





this large could occur due to noise. Nonsignificant lack of fit is good.

The  $F$ -value of the model equal to 17.54 implies the model is significant. There is only a 0.08% chance that a “ $F$ -value” this large could occur due to noise. “ $\text{prob} > F$ ” values less than 0.05 indicate that model terms are significant. In this case,  $A$ ,  $B$ ,  $A^2$  are significant model terms. The “lack of fit  $F$ -value” of 0.79 implies the lack of fit is not significant relative to the pure error. There is a 55.72% chance that a “lack of fit  $F$ -value” this large could occur due to noise. Nonsignificant lack of fit is good.

Based on the obtained results in the ANOVA tables, the  $R^2$  values for the COD and BOD removal percentage are 0.9909 and 0.9261, respectively, which indicate the high reliability of the fitted model. In general,  $R^2$  values above 0.8 indicate that the proposed model is acceptable. The coefficient of variation (CV), which is defined as the ratio of the standard deviation percentage to the mean, is used as a criterion for the repeatability of the models. A model can be defined as repeatable if its CV in our study is less than 10%. Coefficient of variations for COD and TOC removal percentages of 4.87% and 20.89% was calculated, which were acceptable for COD removal. The “pred  $R$ -squared” of 0.9571 is in reasonable agreement with the “adj  $R$ -square” of 0.9844 for COD removal. The “pred  $R$ -squared” of 0.7391 is in reasonable agreement with the “adj  $R$ -square” of 0.8733 for TOC removal.

Equations 1 and 2 show the models fitted with a 95% confidence level to remove COD and TOC

$$\begin{aligned} \text{COD Removal} = & 40.38745 - 10.34721\text{pH} + 1.68677 \\ & \times 10^{-4}\text{Dose} - 3.36700 \times 10^{-6}(\text{Dose} \times \text{pH}) \\ & + 0.78927 \text{pH}^2 - 5.69963 \times 10^{-10}\text{Dose}^2 \end{aligned} \quad (1)$$

$$\begin{aligned} \text{TOC Removal} = & 102.95158 - 27.97060\text{pH} + 1.60920 \\ & \times 10^{-4}\text{Dose} - 1.17845 \times 10^{-6}(\text{Dose} \times \text{pH}) \\ & + 2.06513 \text{pH}^2 - 1.39324 \text{Dose}^2 \end{aligned} \quad (2)$$

Figure 2 shows the experimentally obtained COD and TOC removal percentage values versus the values obtained from the models. As can be seen, the experimentally obtained values are close to the trend line, indicating that the values are near to those obtained from the models.

Figure 3 reveals the perturbation curves for COD and TOC removal. In this figure, the changes of the parameters around the central point are investigated, and it can be considered as a helpful tool for better analysis of contour and 3D surface curves. For both responses, the removal efficiency of COD and TOC decreases initially with increasing solution pH values.

Before reaching the central point, the rate of reduction in efficiency decreases due to the reduction in the slope until the curve changes in the opposite direction. As can be seen, the intensity of the changes in the removal of TOC is greater than that of COD, which is due to the greater slope. The amount of coagulant has also been investigated in these two curves and revealed that the rate of COD and TOC removal efficiency also increases by increasing the coagulant dosage. As depicted in Fig. 2, the slope of the COD removal curve is greater than that of the TOC removal.

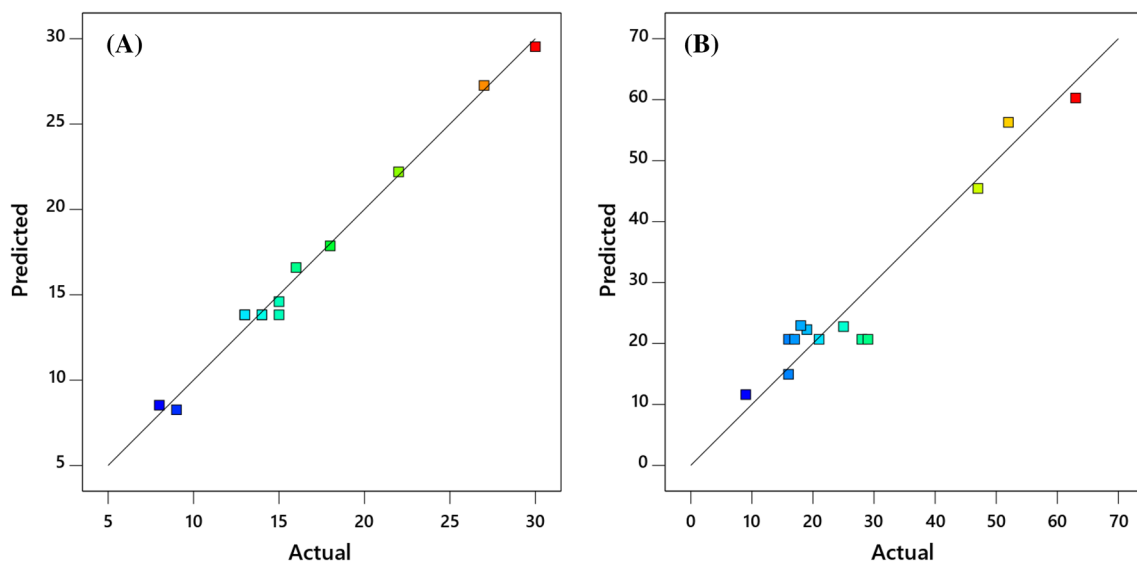


**Fig. 2** Predicted versus actual data obtained by experimental design by RSM. **A** COD removal and **B** TOC removal



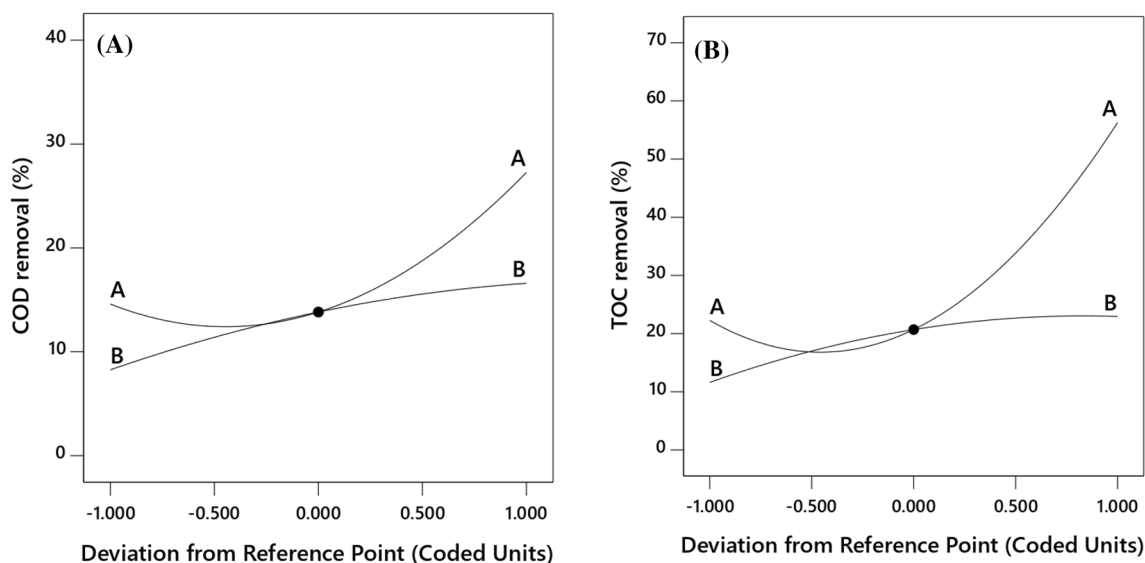


Fig.3 perturbation plots for COD and TOC removal (%) in coagulation and flocculation process: **A** pH (5–11) and **B** FeCl<sub>3</sub> dosage (1–100 gL<sup>-1</sup>)

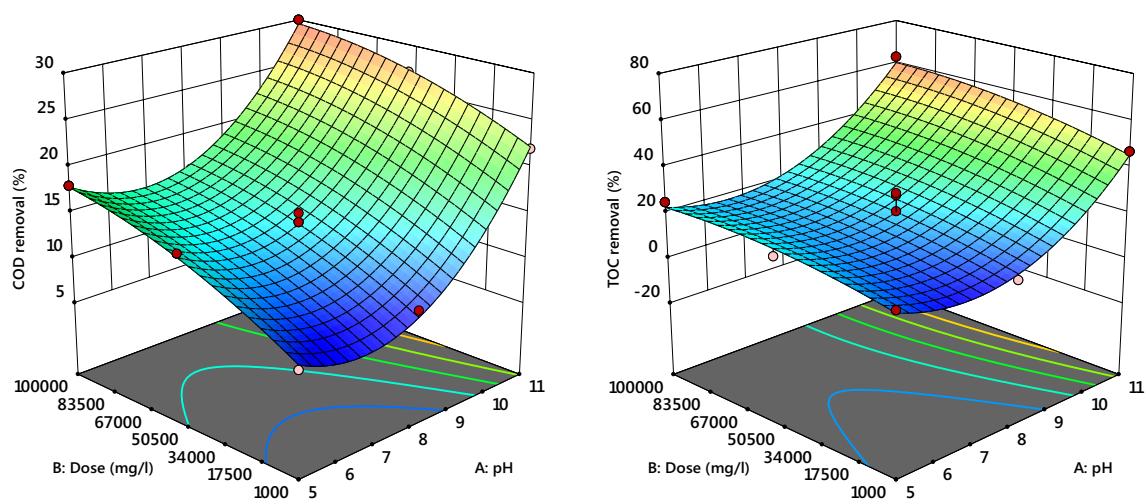


Fig. 4 Three-dimension surface and contour plots for COD and TOC removal effect of pH and coagulant dosage in coagulation and flocculation process

Figure 4 indicates the contour and 3D surface curves. As can be observed, initially with increasing the solution pH, the removal efficiency decreases and then increases, while increasing the amount of coagulant leads to an increase in the removal process efficiency.

**Photo-Fenton process**

After optimizing the conditions for the coagulation and flocculation process by design experiment software and miscellaneous module to find the optimal parameters of the photo-Fenton process, the experiments were designed by central composite module at response surface method. Quantitative

independent parameters included the concentrations of FeSO<sub>4</sub>·7H<sub>2</sub>O and H<sub>2</sub>O<sub>2</sub> (mgL<sup>-1</sup>), and the pH and reaction time (min), which are represented by the letters A, B, C, and D, respectively. Voltage V was considered as a qualitative parameter denoted by the E letter. The experiment was designed to assess the removal percentages of COD and TOC, and out of 60 experiments, 12 were considered as the central point. The reason for using two types of iron compounds in these two processes is to prevent the increase of chloride and sulfate concentrations and their negative effects

**Table 6** Experimental matrix by central composite design and actual responses in COD and TOC removal (%) in photo-Fenton process

Std	Run	A	B	C	D	E	TOC removal efficiency (%)	COD removal efficiency (%)
2	1	46.25	2.19	5.00	33.75	14	34	19
31	2	18.75	2.19	5.00	33.75	14+9	44	20
30	3	32.50	3.13	7.00	62.50	14	53	30
29	4	32.50	3.13	7.00	62.50	14	53	30
56	5	32.50	3.13	7.00	62.50	14+9	53	28
53	6	32.50	3.13	7.00	5.00	14+9	40	24
6	7	46.25	2.19	9.00	33.75	14	31	17
38	8	46.25	4.06	9.00	33.75	14+9	36	20
17	9	5.00	3.13	7.00	62.50	14	68	34
45	10	18.75	4.06	9.00	91.25	14+9	60	30
37	11	18.75	4.06	9.00	33.75	14+9	53	30
39	12	18.75	2.19	5.00	91.25	14+9	49	27
32	13	46.25	2.19	5.00	33.75	14+9	29	17
7	14	18.75	4.06	9.00	33.75	14	48	32
4	15	46.25	4.06	5.00	33.75	14	20	13
19	16	18.75	1.25	7.00	62.50	14	60	28
26	17	32.50	3.13	7.00	62.50	14	55	32
25	18	32.50	3.13	7.00	62.50	14	55	30
15	19	32.50	4.06	9.00	91.25	14	59	30
41	20	32.50	4.06	5.00	92.25	14+9	49	23
33	21	18.75	4.06	5.00	33.75	14+9	45	19
20	22	18.75	5.00	7.00	62.50	14	43	22
11	23	18.75	4.06	5.00	91.25	14	48	21
3	24	32.50	4.06	5.00	33.75	14	50	21
50	25	18.75	5.00	7.00	62.50	14+9	52	25
59	26	18.75	3.13	7.00	62.50	14+9	54	29
49	27	32.50	1.25	7.00	62.50	14+9	43	24
22	28	32.50	3.13	11.00	62.50	14	32	20
35	29	32.50	2.19	9.00	33.75	14+9	36	26
43	30	32.50	2.19	9.00	91.25	14+9	50	29
13	31	18.75	2.19	9.00	91.25	14	59	30
58	32	18.75	3.13	7.00	62.50	14+9	51	30
48	33	18.75	3.13	7.00	62.50	14+9	23	10
60	34	32.50	3.13	7.00	62.50	14+9	54	29
16	35	60.00	4.06	9.00	91.25	14	34	13
18	36	32.50	3.13	7.00	62.50	14	19	8
54	37	46.25	3.13	7.00	120.00	14+9	49	23
55	38	60.00	3.13	7.00	62.50	14+9	53	28
27	39	32.50	3.13	7.00	62.50	14	56	30
5	40	32.50	2.19	9.00	33.75	14	52	33
36	41	32.50	2.19	9.00	33.75	14+9	29	13
9	42	18.75	2.19	5.00	91.25	14	62	29
40	43	46.25	2.19	5.00	91.25	14+9	27	18
51	44	32.50	3.13	3.00	62.50	14+9	20	13
52	45	32.50	3.13	11.00	62.50	14+9	34	21
8	46	46.25	4.06	9.00	33.75	14	25	19
57	47	32.50	3.13	7.00	62.50	14+9	50	28
46	48	46.25	4.06	9.00	91.25	14+9	47	17
23	49	32.50	3.13	7.00	5.00	14	37	26
28	50	32.50	3.13	7.00	62.50	14	54	29



**Table 6** (continued)

Std	Run	A	B	C	D	E	TOC removal efficiency (%)	COD removal efficiency (%)
14	51	46.25	2.19	9.00	91.25	14	44	12
10	52	46.25	2.19	5.00	91.25	14	34	17
44	53	46.25	2.19	9.00	91.25	14+9	36	12
1	54	18.75	2.19	5.00	33.75	14	65	28
42	55	46.25	4.06	5.00	91.25	14+9	25	17
24	56	32.50	3.13	7.00	120.00	14	50	22
12	57	46.25	4.06	5.00	91.25	14	18	11
21	58	32.50	3.13	3.00	62.50	14	28	14
47	59	5.00	3.13	7.00	62.50	14+9	56	30
34	60	46.25	4.06	5.00	33.75	14+9	25	15

(Vedrenne et al. 2012; Xu et al. 2017). The results are presented in Table 6.

According to Table 6, the highest COD removal efficiency was 34%, which was obtained in  $\text{FeSO}_4 \cdot 7\text{H}_2\text{O} = 32.5\text{mgL}^{-1}$ ,  $\text{H}_2\text{O}_2 = 2.19\text{mgL}^{-1}$ , pH=9, reaction time = 33.75 min, and voltage = 14 V. The highest removal efficiency for TOC equal to 68% was also obtained in  $\text{FeSO}_4 \cdot 7\text{H}_2\text{O} = 5\text{mgL}^{-1}$ ,  $\text{H}_2\text{O}_2 = 3.13\text{mgL}^{-1}$ , pH=7, reaction time = 62.5 min, and voltage = 14 V.

In the fit summary section, the cubic vs. quadratic model was considered as the best model for COD removal and the sum of squares, df, mean square, *F*-value, and *P*-value prob > *F* values were, respectively, equal to 10.60 18 0.59 0.75, and 0.7256. However, this model is not usable due to applying lots of parameters. Therefore, the model shown as aliased was discarded and another model proposed by the system was used, which was named quadratic vs 2FI and the sum of squares, df, mean square, *F*-value, and *P*-value prob > *F* values were, respectively, equal to 774.77, 4, 193.69, 279.03, and < 0.0001. For TOC removal, it is stated in the fit summary section that the cubic vs quadratic model is the best because the sum of squares, df, mean square, *F*-value, and *P*-value prob > *F* parameters are 53.81, 18 2.99, 1.05, and 0.4541, respectively. For the reasons given earlier, the model shown as aliased is discarded and the model proposed by the system, which was named quadratic vs 2FI with the sum of squares, df, mean square, *F*-value, and *P*-value prob > *F* values, respectively, equal to 2411.94, 4, 602.98, 206.78, and < 0.0001, is considered. Additional information about the fitted model is presented in Tables 7 and 8.

The *F*-value of 210.25 implies that the model is significant. There is only a 0.01% chance that a “*F*-value” this large could occur due to noise. Values of “prob > *F*” less than 0.05

indicate that model terms are significant. In the case of A, B, C, D, E, AB, AC, AD, AE, BC, BE, CD, and DE,  $A^2$ ,  $B^2$ ,  $C^2$ ,  $D^2$  are significant model terms. The “lack of fit *F*-value” of 0.80 implies that the lack of fit is not significant relative to the pure error. There is a 69.86% chance that a “lack of fit *F*-value” this large could occur due to noise. Nonsignificant lack of fit is good.

The *F*-value of 177.47 implies that the model is significant. There is only a 0.01% chance that a “*F*-value” this large could occur due to noise. Values of “prob > *F*” less than 0.05 indicate that the model terms are significant. In the case of A, B, C, D, E, AB, AC, AD, AE, BC, BE, CD, and DE,  $A^2$ ,  $B^2$ ,  $C^2$ ,  $D^2$  are significant model terms. The “lack of fit *F*-value” of 1.53 implies that the lack of fit is not significant relative to the pure error. There is a 24.23% chance that a “lack of fit *F*-value” this large could occur due to noise. Nonsignificant lack of fit is good.

Based on obtained results in the ANOVA table, the correlation coefficients ( $R^2$ ) for the calculation of the COD and TOC removal were 0.9901 and 0.9883, respectively, which indicates the high reliability of the fitted model. The CV percentages for calculating the COD and TOC removal efficiencies were 3.63% and 3.91%, respectively, which is less than 10% for both models and indicates its repeatability.

The “pred *R*-squared” of 0.9783 is in reasonable agreement with the “adj *R*-square” of 0.9854 for COD removal.

The “pred *R*-squared” of 0.9715 is in reasonable agreement with the “adj *R*-square” of 0.9827 for TOC removal.

Equations below show fitted models with a 95% confidence level to removing COD and TOC at 14 and 14 + 9 Volts.



14 V	<p>COD removal = <math>-29.12158 + 0.77284 \text{ FeSO}_4 + 0.21323 \text{ H}_2\text{O}_2 + 12.12792 \text{ pH} + 0.38922 \text{ Time} + 0.033939 (\text{FeSO}_4 \times \text{H}_2\text{O}_2) - 0.061364 (\text{FeSO}_4 \times \text{pH}) - 2.21344 \times 10^{-3} (\text{FeSO}_4 \times \text{Time}) - 6.95652 \times 10^{-3} (\text{H}_2\text{O}_2 \times \text{Time}) + 0.8666 7 (\text{H}_2\text{O}_2 \times \text{pH}) - 0.016304 (\text{pH} \times \text{Time}) - 0.012011 (\text{FeSO}_4)^2 - 1.37481 (\text{H}_2\text{O}_2)^2 - 0.78646 (\text{pH})^2 - 1.76434 \times 10^{-3} \times (\text{Time})^2</math></p> <p>TOC removal = <math>+37.83574 - 0.17034 \text{ FeSO}_4 - 7.23665 \text{ H}_2\text{O}_2 + 12.48632 \text{ pH} + 0.16117 \text{ Time} - 0.070303 (\text{FeSO}_4 \times \text{H}_2\text{O}_2) - 0.073864 (\text{FeSO}_4 \times \text{pH}) - 5.5336 0 \times 10^{-4} (\text{FeSO}_4 \times \text{Time}) + 1.483 33 (\text{H}_2\text{O}_2 \times \text{pH}) - 3.47826 \times 10^{-3} (\text{H}_2\text{O}_2 \times \text{Time}) + 0.042935 (\text{Time} \times \text{pH}) - 0.015455 (\text{FeSO}_4)^2 - 0.90667 (\text{H}_2\text{O}_2)^2 - 1.54297 (\text{pH})^2 - 2.77883 \times 10^{-3} \times (\text{Time})^2</math></p>	9 + 14 V	<p>COD removal = <math>-43.67437 + 0.90012 \text{ FeSO}_4 + 2.25768 \text{ H}_2\text{O}_2 + 12.12792 \text{ pH} + 0.44139 \text{ Time} + 0.033939 (\text{FeSO}_4 \times \text{H}_2\text{O}_2) - 0.061364 (\text{FeSO}_4 \times \text{pH}) - 2.21344 \times 10^{-3} (\text{FeSO}_4 \times \text{Time}) - 6.95652 \times 10^{-3} (\text{H}_2\text{O}_2 \times \text{Time}) + 0.8666 7 (\text{H}_2\text{O}_2 \times \text{pH}) - 0.016304 (\text{pH} \times \text{Time}) - 0.012011 (\text{FeSO}_4)^2 - 1.37481 (\text{H}_2\text{O}_2)^2 - 0.78646 (\text{pH})^2 - 1.76434 \times 10^{-3} \times (\text{Time})^2</math></p> <p>TOC removal = <math>-7.19582 - 0.14178 \text{ FeSO}_4 - 0.54113 \text{ H}_2\text{O}_2 + 13.59049 \text{ pH} + 0.16842 \text{ Time} - 0.070303 (\text{FeSO}_4 \times \text{H}_2\text{O}_2) - 0.073864 (\text{FeSO}_4 \times \text{pH}) - 5.53360 \times 10^{-4} (\text{FeSO}_4 \times \text{Time}) + 1.48333 (\text{H}_2\text{O}_2 \times \text{pH}) - 3.47826 \times 10^{-3} (\text{H}_2\text{O}_2 \times \text{Time}) + 0.042935 (\text{Time} \times \text{pH}) - 0.015455 (\text{FeSO}_4)^2 - 0.90667 (\text{H}_2\text{O}_2)^2 - 1.54297 (\text{pH})^2 - 2.77883 \times 10^{-3} \times (\text{Time})^2</math></p>
------	--	----------	---

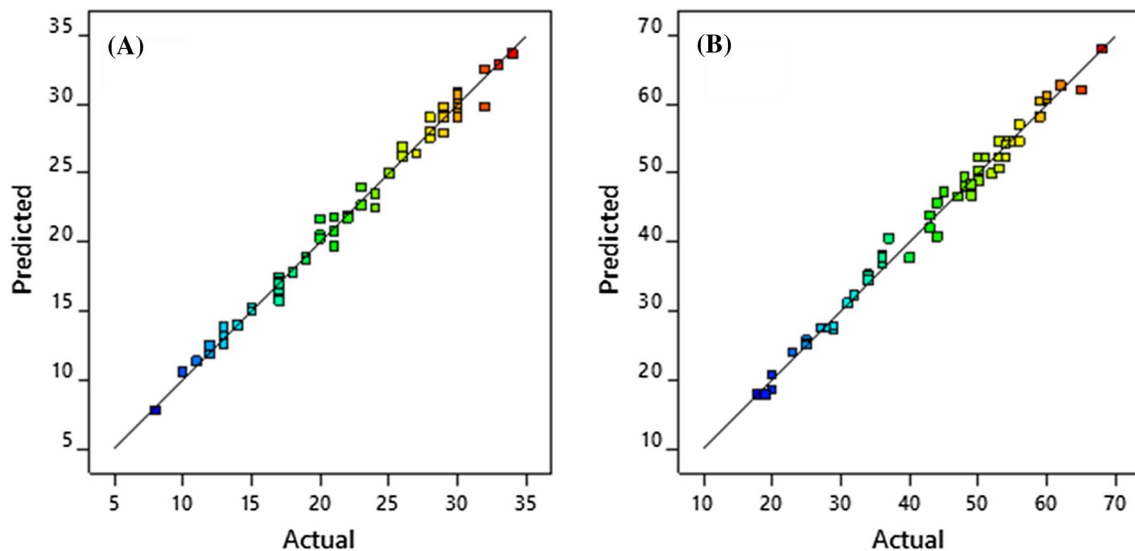
Figure 5 reveals the COD and TOC removal percentages obtained through laboratory experiments versus the values obtained from the RSM models in photo-Fenton process. As can be seen, the values attained experimentally are closer

**Table 7** ANOVA test for response surface quadratic model for COD removal (%) in photo-Fenton process

Source	Sum of squares	df	Mean square	F-value	p-value	
Model	2773.08	19	145.95	210.25	<0.0001	Significant
A-FeSO <sub>4</sub> + 7H <sub>2</sub> O	1496.33	1	1496.33	2155.58	<0.0001	
B-H <sub>2</sub> O <sub>2</sub>	16.33	1	16.33	23.53	<0.0001	
C-pH	126.75	1	126.75	182.59	<0.0001	
D-Time	6.75	1	6.75	9.72	0.0034	
E-voltage	8.82	1	8.82	12.70	0.0010	
AB	6.13	1	6.13	8.82	0.0050	
AC	91.12	1	91.12	131.27	<0.0001	
AD	24.50	1	24.50	35.29	<0.0001	
AE	36.75	1	36.75	52.94	<0.0001	
BC	84.50	1	84.50	121.73	<0.0001	
BD	1.13	1	1.13	1.62	0.2104	
BE	44.08	1	44.08	63.51	<0.0001	
CD	28.12	1	28.12	40.52	<0.0001	
CE	0.0000	1	0.0000	0.0000	1.0000	
DE	27.00	1	27.00	38.90	<0.0001	
A <sup>2</sup>	282.88	1	282.88	407.51	<0.0001	
B <sup>2</sup>	80.10	1	80.10	115.38	<0.0001	
C <sup>2</sup>	542.88	1	542.88	782.06	<0.0001	
D <sup>2</sup>	116.67	1	116.67	168.07	<0.0001	
Residual	27.77	40	0.6942			
Lack of fit	19.60	30	0.6533	0.8000	0.6986	Not significant
Pure error	8.17	10	0.8167			
Cor total	2800.85	59				

**Table 8** ANOVA test for response surface quadratic model for TOC removal (%) in photo-Fenton process

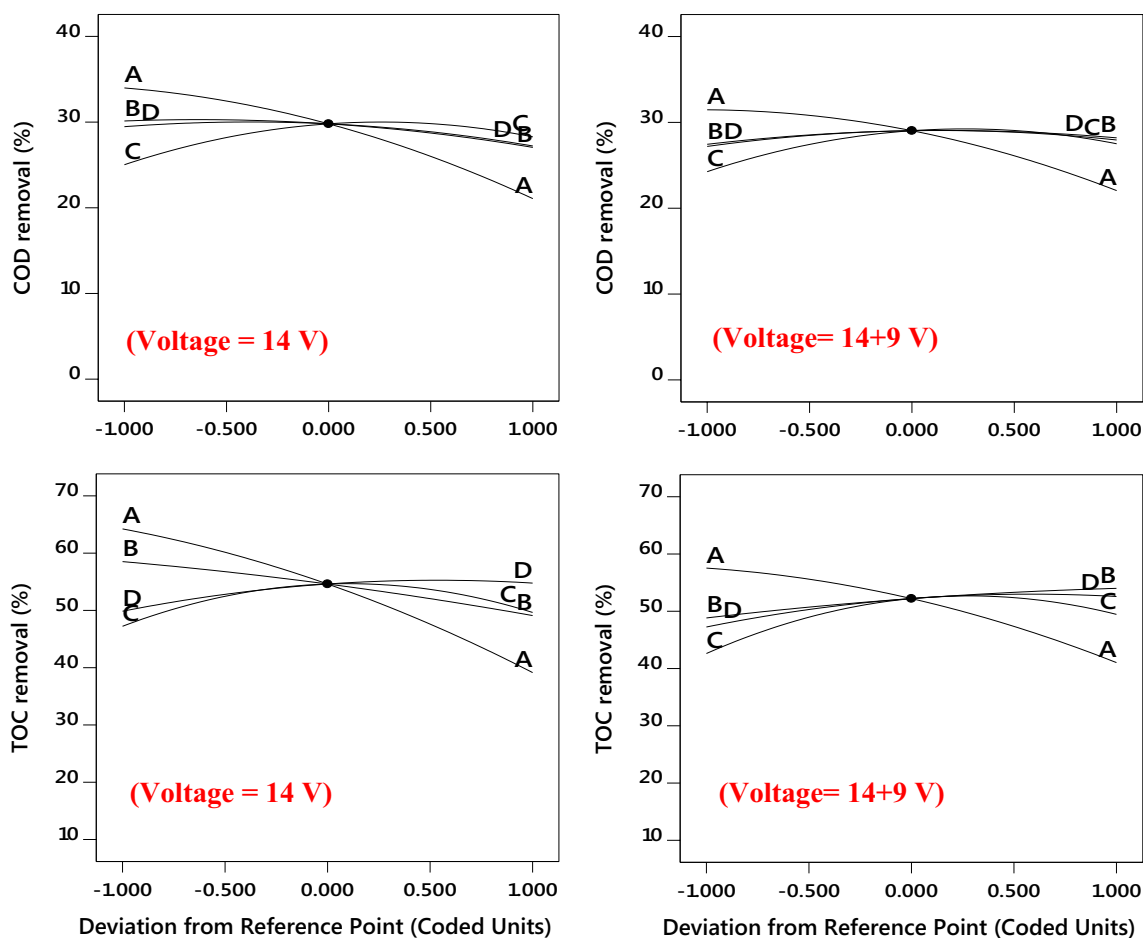
Source	Sum of squares	df	Mean square	F-value	p-value	
Model	9832.69	19	517.51	177.47	<0.0001	Significant
A-FeSO <sub>4</sub> +7H <sub>2</sub> O	5187.52	1	5187.52	1778.96	<0.0001	
B-H <sub>2</sub> O <sub>2</sub>	54.19	1	54.19	18.58	0.0001	
C-pH	256.69	1	256.69	88.03	<0.0001	
D-Time	315.19	1	315.19	108.09	<0.0001	
E-voltage	86.40	1	86.40	29.63	<0.0001	
AB	26.28	1	26.28	9.01	0.0046	
AC	132.03	1	132.03	45.28	<0.0001	
AD	1.53	1	1.53	0.5251	0.4729	
AE	221.02	1	221.02	75.79	<0.0001	
BC	247.53	1	247.53	84.89	<0.0001	
BD	0.2813	1	0.2813	0.0964	0.7577	
BE	638.02	1	638.02	218.80	<0.0001	
CD	195.03	1	195.03	66.88	<0.0001	
CE	58.52	1	58.52	20.07	<0.0001	
DE	0.5208	1	0.5208	0.1786	0.6748	
A <sup>2</sup>	468.33	1	468.33	160.61	<0.0001	
B <sup>2</sup>	34.83	1	34.83	11.95	0.0013	
C <sup>2</sup>	2089.62	1	2089.62	716.59	<0.0001	
D <sup>2</sup>	289.41	1	289.41	99.25	<0.0001	
Residual	116.64	40	2.92			
Lack of fit	95.81	30	3.19	1.53	0.2423	Not significant
Pure error	20.83	10	2.08			
Cor total	9949.33	59				

**Fig. 5** Predicted versus actual data obtained by experimental design by RSM in photo-Fenton process **A** COD removal and **B** TOC removal

to the straight line, which can be assumed that the values obtained experimentally are close to the values obtained from the models. In addition, Fig. 5 shows that the COD removal percentage results were more consistent than TOC.

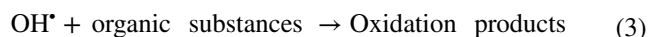
Figure 6 shows the perturbation curves of the COD and TOC removal percentages. In these curves, the changes of the parameters around the central point at 14 and 14 + 9 V are examined, which can be considered as a subsidiary tool for analyzing contour and 3D surface curves. According to





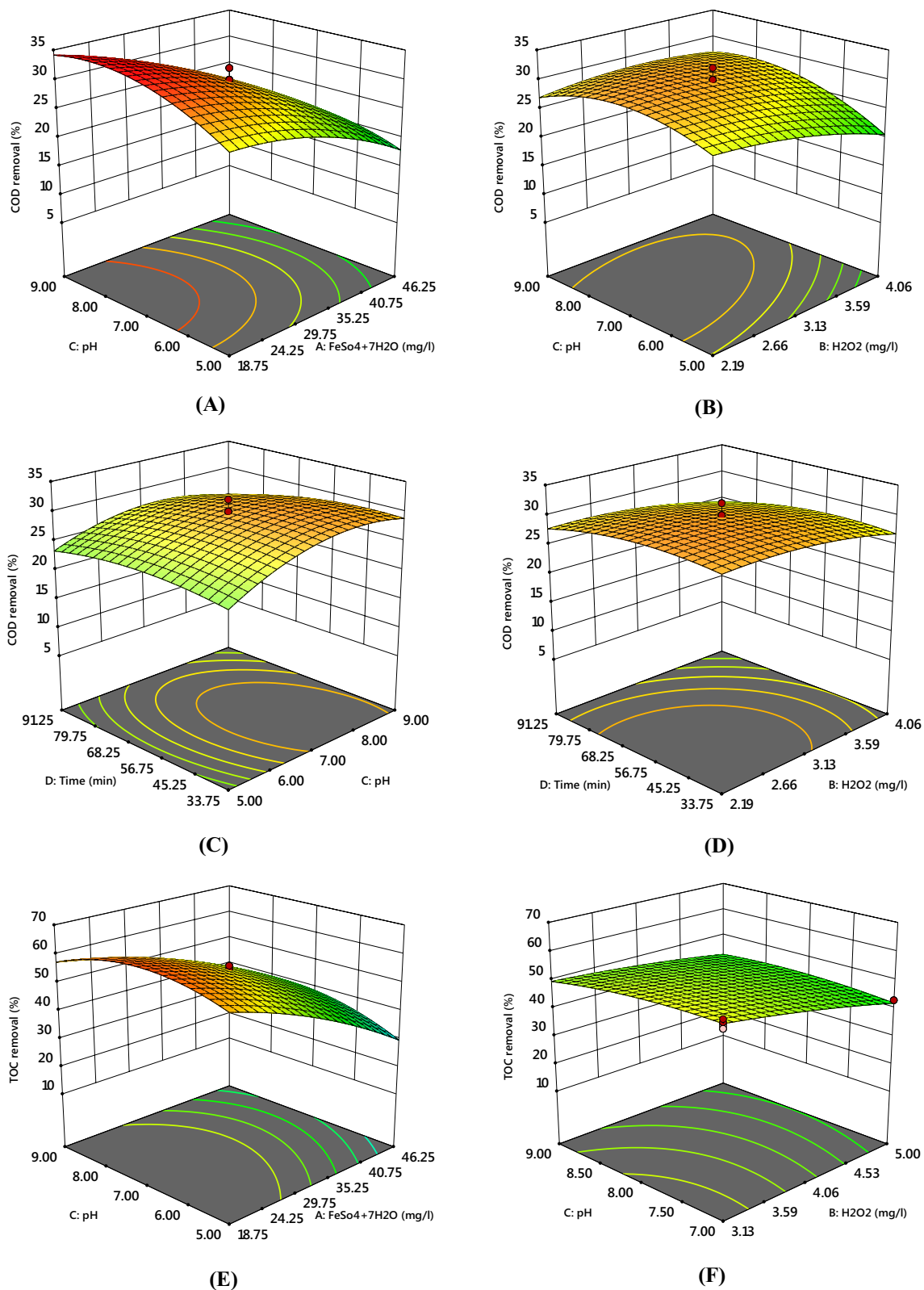
**Fig. 6** Perturbation plots for COD and TOC removal (%) in photo-Fenton process at 14 and 14+9 V t: **A**  $\text{FeSO}_4$  (5–60  $\text{mg mL}^{-1}$ ), **B**  $\text{H}_2\text{O}_2$  (1.25–5  $\text{mgL}^{-1}$ ), **C** pH (3–11), and **D** time (5–120 min)

Fig. 5 for both responses, the removal efficiency decreases with the increasing amount of  $\text{FeSO}_4 \cdot 7\text{H}_2\text{O}$ , which can be due to the conversion of  $\text{Fe}^{+2}$  to  $\text{Fe}^{+3}$ , which ultimately increases water turbidity and reduction of light penetration. As depicted, the curve slope at voltage 14 is higher than 14+9 V, which can be deduced that the changes of the variables at 14 V are more obvious in the COD and TOC removal. COD removal percentages in different amounts of  $\text{H}_2\text{O}_2$  at 14+9 V show a steady trend, but at 14 V with a slight slope with increasing  $\text{H}_2\text{O}_2$  the removal percentage decreases. The effect of increasing hydrogen peroxide is such that at 14+9 V the TOC removal percentage increases with a slight slope, while at 14 V, the removal percentage decreases with a greater slope. The oxidation of organic substances in the leachate by hydroxyl radicals produced from a reaction between  $\text{H}_2\text{O}_2$  and iron followed the reaction below (Eq. 3) (Roudi et al. 2021).



The effect of pH was also investigated at voltages 14 and 14+9 V, and it was found that with increasing the solution pH, the removal efficiency of COD and TOC first increases and then decreases, which is more evident in voltage 14 V. The reaction time also affects the COD and TOC removal efficiency in such a way that by increasing this parameter, the removal percentage increases slightly, which is more intense at 14+9 V.

In order to determine the effect of the studied parameters on each other and better understand the perturbation diagrams, the results of this step are shown in Fig. 7 by 3D and contour diagrams.



**Fig. 7** Three-dimension surface and contour plots for COD and TOC removal (%) **A E** Effect of pH and FeSO<sub>4</sub> at H<sub>2</sub>O<sub>2</sub> (mgL<sup>-1</sup>)=3.13, time (min)=62.50, voltage (V)=14 **B F** Effect of pH and H<sub>2</sub>O<sub>2</sub> at FeSO<sub>4</sub> (mgL<sup>-1</sup>)=32.50, time (min)=62.50, voltage (V)=14 **C G**

Effect of time and pH at FeSO<sub>4</sub> (mgL<sup>-1</sup>)=32.50 H<sub>2</sub>O<sub>2</sub> (mgL<sup>-1</sup>)=3.13, voltage (V)=14 **D H** Effect of time and H<sub>2</sub>O<sub>2</sub> at FeSO<sub>4</sub> (mgL<sup>-1</sup>)=32.50, pH=7, voltage (V)=14

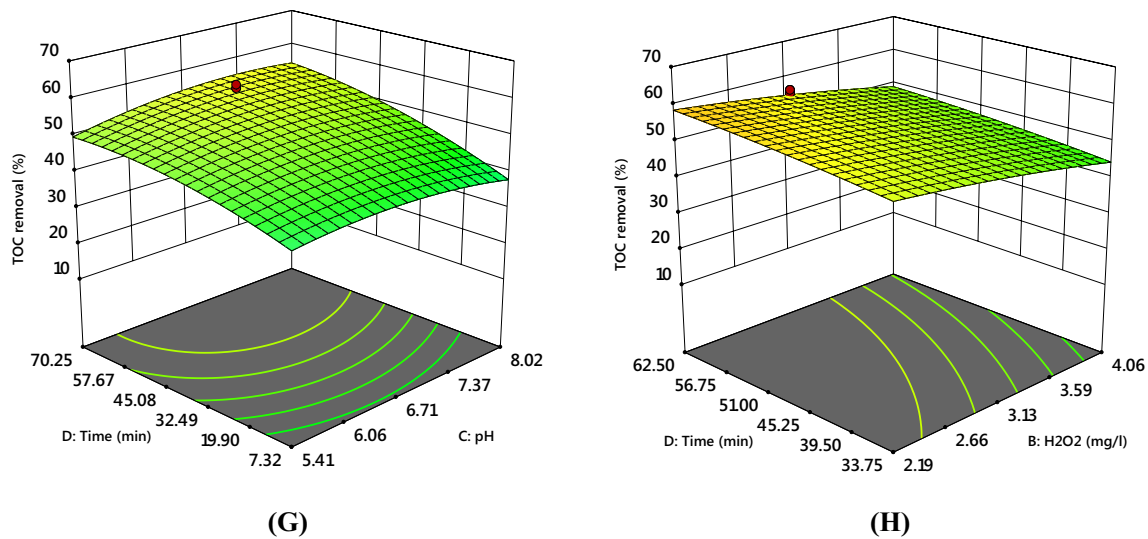


Fig. 7 (continued)

## Biological process

As mentioned, initially leachate had little opportunity for biodegradation due to its low  $BOD_5/COD$  ratio. However, after the supernatant was treated by coagulation–flocculation and photo-Fenton processes, this ratio reached above 0.4 indicating that organic materials in addition to being converted to water and carbon dioxide can be decomposed into the biodegradable materials. Figure 8 reveals a comparison of two treated leachates with extensive aeration (EA) and a hybrid process (CF/PF/EA). Based on this figure, when the extensive aeration process is used, the COD removal percentage in the biological reactor over 72 h is 25%, while this parameter at the same time is equal to 85% for the hybrid process. Figure 8 shows that after 24 h, the COD/COD<sub>0</sub> ratio was reduced to half from around 1 and reached 0.2 after 72 h, which shows the effectiveness of the hybrid process (CF/PF) as pretreatment of Extended aeration.

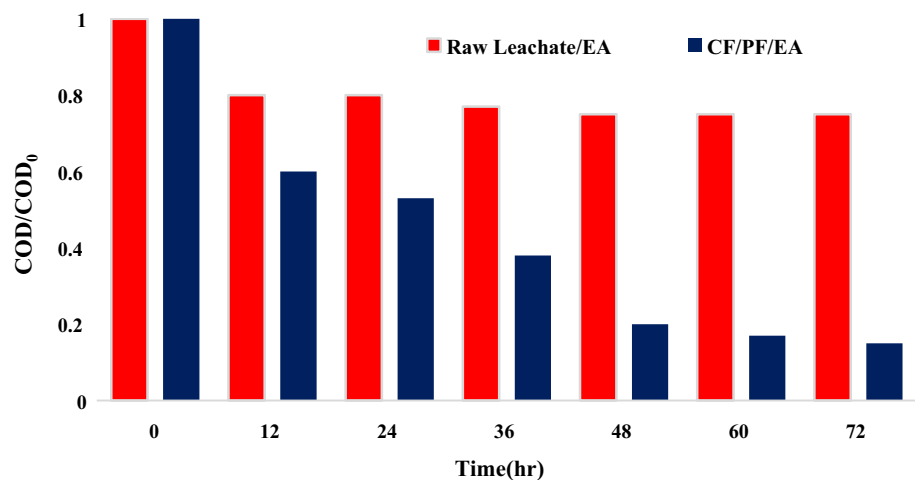
According to the obtained results, sludge bacteria from the hybrid process have a greater ability to remove organic compounds, which can be attributed to the ability to convert complex organic materials into simpler materials. In addition, the slope line of the hybrid process (Fig. 7) is greater than the EA process, which indicates that the decomposition rate of organic materials by bacteria in the resulting leachate is higher than that of the raw leachate. It was also found that raw leachate bacteria lose their ability to decompose organic materials after 36 h, whereas this action lasts up to 72 h by bacteria in the hybrid process (relaxation time).

## Conclusion

The management of mature leachate is difficult due to the presence of non-biodegradable materials, so this problem can be overcome to some extent by using physicochemical method. This study examined hybrid processes (CF/PF) and their interaction using response surface methodology (RSM) with central composite design and how they affected the treatment of landfill leachate with extended aeration. Coagulation and flocculation experiments were designed by miscellaneous module, and then, the central composite module was used to design experiments in the photo-Fenton process. Coagulation and flocculation process had advantages such as increasing light penetration due to reducing water, coloring, turbidity, and the amount of sludge produced, which have increased the efficiency of the photo-Fenton process. Using CF process initially led to the removal efficiencies of 30% COD and 63% TOC at pH 11 and coagulant dosage of  $100 \text{ gL}^{-1}$ . Then, in the photo-Fenton process removal efficiencies of 34% COD and 68% TOC were obtained (at pH = 7 coagulant dosage =  $5 \text{ mgL}^{-1}$   $H_2O_2 = 3.13 \text{ mgL}^{-1}$  reaction time = 62.5 min and voltage = 14 V). The correlation coefficients ( $R^2$ ) obtained in the coagulation and flocculation process for removing COD and TOC were equal to 0.9909 and 0.9261, respectively, while in the photo-Fenton process was 0.9901 for COD removal and 0.9881 for TOC removal. Treated leachate resulting from the hybrid process was biologically treated for 72 h to evaluate the effectiveness of this process. The COD removal percentage before and after the



**Fig. 8** Comparing the yield of COD removal from leachate using only the extended aeration (EA) process vs. hybrid process consist of coagulation and flocculation, photo-Fenton and extended aeration (CF/PF/EA).



hybrid process was 25% and 85%, respectively. The COD/COD<sub>0</sub> ratio decreased from about 1 in the extended aeration process to 0.2 in the hybrid processes after 72 h, which reveals the effectiveness of the CF/PF processes. According to the results, the combination of the coagulation and flocculation photo-Fenton and extended aeration could be considered as an efficient strategy in leachate treatment.

**Acknowledgments** The authors wish to thank all who assisted in conducting this work.

## Declarations

**Conflict of interest** The authors declare that they have no conflict of interest.

## References

- Amor C, Torres-Sociás ED, Peres JA, Maldonado MI, Oller I, Malato S, Lucas MS (2015) Mature landfill leachate treatment by coagulation/flocculation combined with fenton and solar photo-fenton processes. *J Hazard Mater* 286:261–268. <https://doi.org/10.1016/j.jhazmat.2014.12.036>
- Anna Tałałaj I, Bartkowska I, Biedka P (2021) Treatment of young and stabilized landfill leachate by integrated sequencing batch reactor (sbr) and reverse osmosis (ro) process. *Environ Nanotechnol Monit Manag* 16:100502. <https://doi.org/10.1016/j.enmm.2021.100502>
- Behnezhad M, Hashemzadeh F, Hassani AM (2021) Investigation on the effect of ozonation process before and after coagulation on reduction in leachate pollutants. *Desalin Water Treat.* <https://doi.org/10.5004/dwt.2021.26480>
- Cheng SY, Show P-L, Juan JC, Chang J-S, Lau BF, Lai SH, Ng EP, Yian HC, Ling TC (2021) Landfill leachate wastewater treatment to facilitate resource recovery by a coagulation-flocculation process via hydrogen bond. *Chemosphere* 262:127829. <https://doi.org/10.1016/j.chemosphere.2020.127829>
- Colombo A, Módenes AN, Góes Trigueros DE, Giordani da Costa SI, Borba FH, Espinoza-Quiñones FR (2019) Treatment of sanitary landfill leachate by the combination of photo-fenton and biological processes. *J Clean Prod* 214:145–153. <https://doi.org/10.1016/j.jclepro.2018.12.310>
- de Morais JL, Zamora PP (2005) Use of advanced oxidation processes to improve the biodegradability of mature landfill leachates. *J Hazard Mater* 123(1):181–186. <https://doi.org/10.1016/j.jhazmat.2005.03.041>
- Jiang K, Cheng Z, Lou Z, Wang L, Lu H, Xu B, Jin N (2021) Chemical and olfactive impacts of organic matters on odor emission patterns from the simulated construction and demolition waste landfills. *J Environ Sci* 103:196–206. <https://doi.org/10.1016/j.jes.2020.10.016>. (AnitaMaslahatiRoudi2021)
- Kawai M, Kishi M, Hamersley MR, Nagao N, Hermana J, Toda T (2012) Biodegradability and methane productivity during anaerobic co-digestion of refractory leachate. *Int Biodeterior Biodegrad* 72:46–51. <https://doi.org/10.1016/j.ibiod.2012.04.003>
- Kurtoğlu Akkaya G, Bilgili MS (2020) Evaluating the performance of an electro-membrane bioreactor in treatment of young leachate. *J Environ Chem Eng* 8(4):104017. <https://doi.org/10.1016/j.jece.2020.104017>
- Kusworo TD, Kumoro AC, Utomo DP (2021) Phenol and ammonia removal in petroleum refinery wastewater using a poly(vinyl) alcohol coated polysulfone nanohybrid membrane. *J Water Process Eng* 39:101718. <https://doi.org/10.1016/j.jwpe.2020.101718>
- Li J, Zhao L, Qin L, Tian X, Wang A, Zhou Y, Meng L, Chen Y (2016) Removal of refractory organics in nanofiltration concentrates of municipal solid waste leachate treatment plants by combined fenton oxidative-coagulation with photo-fenton processes. *Chemosphere* 146:442–449. <https://doi.org/10.1016/j.chemosphere.2015.12.069>
- Liu J, Gu Z, Wang X, Li Q (2022) The molecular differences of young and mature landfill leachates: Molecular composition chemical property and structural characteristic. *Chemosphere* 287:132215. <https://doi.org/10.1016/j.chemosphere.2021.132215>
- Mirghorayshi M, Zinatizadeh AA, van Loosdrecht M (2021) Simultaneous biodegradability enhancement and high-efficient nitrogen removal in an innovative single stage anaerobic/anoxic/aerobic hybrid airlift bioreactor (HALBR) for composting leachate treatment: process modeling and optimization. *Chem Eng J* 407:127019. <https://doi.org/10.1016/j.cej.2020.127019>
- Nain A, Lohchab RK, Singh K, Kumari M, Saini JK (2021) MSW stabilization in an anaerobic bioreactor landfill and evaluation of in-situ leachate treatment potential with the help of quadric model. *J Mater Cycles Waste Manage* 23(6):2192–2207. <https://doi.org/10.1007/s10163-021-01287-4>



- Peng Y (2017) Perspectives on technology for landfill leachate treatment. *Arab J Chem* 10:S2567–S2574. <https://doi.org/10.1016/j.arabjc.2013.09.031>
- Pisharody L, Gopinath A, Malhotra M, Nidheesh PV, Kumar MS (2022) Occurrence of organic micropollutants in municipal landfill leachate and its effective treatment by advanced oxidation processes. *Chemosphere* 287:132216. <https://doi.org/10.1016/j.chemosphere.2021.132216>
- Roudi AM, Salem S, Abedini M, Maslahati A, Imran M (2021) Response surface methodology (RSM)-based prediction and optimization of the fenton process in landfill leachate decolorization. *Processes* 9(12):2284. <https://doi.org/10.3390/pr9122284>
- Sawamura H, Yamada M, Endo K, Soda S, Ishigaki T, Ike M (2010) Characterization of microorganisms at different landfill depths using carbon-utilization patterns and 16s rRNA gene based t-rflp. *J Biosci Bioeng* 109(2):130–137. <https://doi.org/10.1016/j.jbiosc.2009.07.020>
- Shi L, Chen H, Meng H, Cheng R, Dai J, Zheng X, Zhang Z (2021) How environmental policy impacts technology adoption: a case of landfill leachate. *J Clean Prod* 310:127484. <https://doi.org/10.1016/j.jclepro.2021.127484>
- Singh SK, Tang WZ (2013) Statistical analysis of optimum fenton oxidation conditions for landfill leachate treatment. *Waste Manage* 33(1):81–88. <https://doi.org/10.1016/j.wasman.2012.08.005>
- Tejera J, Hermosilla D, Gascó A, Miranda R, Alonso V, Negro C, Blanco Á (2021) Treatment of mature landfill leachate by electrocoagulation followed by fenton or uva-led photo-fenton processes. *J Taiwan Inst Chem Eng* 119:33–44. <https://doi.org/10.1016/j.jtice.2021.02.018>
- Vedrenne M, Vasquez-Medrano R, Prato-Garcia D, Frontana-Uribe BA, Ibanez JG (2012) Characterization and detoxification of a mature landfill leachate using a combined coagulation–flocculation/photo fenton treatment. *J Hazard Mater* 205–206:208–215. <https://doi.org/10.1016/j.jhazmat.2011.12.060>
- Veli S, Arslan A, Isgoren M, Bingöl D, Demiral D (2021) Experimental design approach to COD and color removal of landfill leachate by the electrooxidation process. *Environ Chall*. <https://doi.org/10.1016/j.envc.2021.100369>
- Vilar VJP, Rocha EMR, Mota FS, Fonseca A, Saraiva I, Boaventura RAR (2011) Treatment of a sanitary landfill leachate using combined solar photo-fenton and biological immobilized biomass reactor at a pilot scale. *Water Res* 45(8):2647–2658. <https://doi.org/10.1016/j.watres.2011.02.019>
- Wijekoon P, Koliyabandara PA, Cooray AT, Lam SS, Athapattu BCL, Vithanage M (2022) Progress and prospects in mitigation of landfill leachate pollution: risk pollution potential treatment and challenges. *J Hazard Mater* 421:126627. <https://doi.org/10.1016/j.jhazmat.2021.126627>
- Wu C, Chen W, Gu Z, Li Q (2021) A review of the characteristics of fenton and ozonation systems in landfill leachate treatment. *Sci Total Environ* 762:143131. <https://doi.org/10.1016/j.scitotenv.2020.143131>
- Xu J, Long Y, Shen D, Feng H, Chen T (2017) Optimization of fenton treatment process for degradation of refractory organics in pre-coagulated leachate membrane concentrates. *J Hazard Mater* 323:674–680. <https://doi.org/10.1016/j.jhazmat.2016.10.031>
- Yang X, De Buyck P-J, Zhang R, Manhaeghe D, Wang H, Chen L, Zhao Y, Demeestere K, Van Hulle SWH (2022) Enhanced removal of refractory humic- and fulvic-like organics from biotreated landfill leachate by ozonation in packed bubble columns. *Sci Total Environ* 807:150762. <https://doi.org/10.1016/j.scitotenv.2021.150762>
- Zhao R, Liu J, Feng J, Li X, Li B (2021) Microbial community composition and metabolic functions in landfill leachate from different landfills of China. *Sci Total Environ* 767:144861. <https://doi.org/10.1016/j.scitotenv.2020.144861>
- Zielińska M, Kulikowska D, Stańczak M (2020) Adsorption — membrane process for treatment of stabilized municipal landfill leachate. *Waste Manage* 114:174–182. <https://doi.org/10.1016/j.wasman.2020.07.011>

Springer Nature or its licensor (e.g. a society or other partner) holds exclusive rights to this article under a publishing agreement with the author(s) or other rightsholder(s); author self-archiving of the accepted manuscript version of this article is solely governed by the terms of such publishing agreement and applicable law.

